Astro 518 Term Paper

Comparison of Spitzer IRAC and JWST NIRCam

Yifan Zhou

University of Arizona

yifzhou@email.arizona.edu

1. Introduction

Infrared Array Camera (IRAC) is the near infrared imaging instrument equipped on Spitzer Space Telescope. NIRCam is the imaging camera on James Webb Space Telescope (JWST). I listed the general design of these instruments and compared their performance.

Although exoplanet observation is not the key factor in defining the IRAC desgin (Fazio et al. 2004), astronomers made great progress in detecting and characterizing exoplanet with the help of IRAC. I listed several key discoveries in exoplanet with IRAC to demonstrate what features of IRAC is employed in exoplanet studies. With the performance comparison, we can see the potential of NIRCam in exoplanet observations.

2. Instrumentation Design

2.1. Optical Design

The optical design of Spitzer IRAC and JWST NIRCam are demonstrated in figure 1.

2.1.1. IRAC

The optics path of IRAC is relatively simple comparing to that of NIRCam. Two pickoff mirrors that are slightly displaced and tilted separate the light into two beams. Each reflected beam then passes doublet lenses and is reimaged at the focal plane. After the doublet lenses, two Ge substrate beam splitters separate the lower beam into Channel 1 (reflected) and Channel 3 (transmitted) and the upper beam into Channel 2 (reflected) and Channel 4 (transmitted). Finally 4 Channels of light are received by 4 detectors accordingly (Fazio et al. 2004).

2.1.2. NIRCam

NIRCam consists of two modules, each imaging a $2.16' \times 2.16'$ field of view. The modules are built on two optical benches mounted back-to-back. As a result, the two fields of views imaged by the modules are adjacent. The modules are functionally identical, with identical optical and focal plane components. They are mirror images of each other except for coronagraphic pupil masks (Huff 2005).

The optical design of each module is shown in the lower panel of figure 1. Comparing to IRAC, more devices are deployed on the optics path of NIRCam so that different types of observation can be accomplished. After reflection of pickoff mirror and first fold mirror, the light are then split by a dichroic beam-splitter into long wave beam and short wave beam. Before the two beams reach the detectors, two filter wheels are equipped on the paths to enable multi-band imaging observation. After the pick-off mirror, there is a coronagraph elements to provide NIRCam the ability to make coronagraphic measurements. NIRCam also has a grism to work on spectroscopic observation.

Several optical elements are added or specially designed for optical accuracy improve-

ment. The pickoff mirror is actuated by a three degree-of- freedom focus and alignment mechanism that provides fine positioning in tip, tilt, and piston, allowing NIRCam to accommodate small pointing and focus changes that may manifest themselves once the observatory is on-orbit (Huff 2005). Internal calibration sources including a flat field source and a coranographic source are used to aid with on-orbit calibration and characterization.

2.2. Focal Plane Array

2.2.1. IRAC

IRAC has 4 detector arrays to receive photons in 4 channels. The 4 arrays are all 256×256 pixels in size and have the same physical pixel size of 30 μm. The channel 1 and channel 2 arrays are made of InSb while the longer wavelength channels 3 and 4 are Si:As detectors(Fazio et al. 2004).

2.2.2. NIRCam

NIRCam is based on 2048×2048 HgCdTe photodiode chips, with physical pixel size of 18 μm × 18 μm pixels (Burriesci 2005). The chips used for the short and long wavelength channels are based on different types of HgCdTe. However, in what concerns their functionality and control they are basically identical. The sensitive area of a chip is 2040x2040 pixels, due to a 4 pixel wide border of reference pixels along all edges. Reference pixels are used for tracking bias drifts during an exposure. The finer pixel scale of the short-wavelength channels requires a Focal Plane Array, i.e. a 2×2 mosaic of chips butted with a small gap ($5''$) between them (Burriesci 2005). The resulting gaps in the images have to be filled by dithering moves of the telescope. The long wavelength channels use a single chip. The fields observed by the two modules are adjacent with about $50''$ separation. Also this larger gap

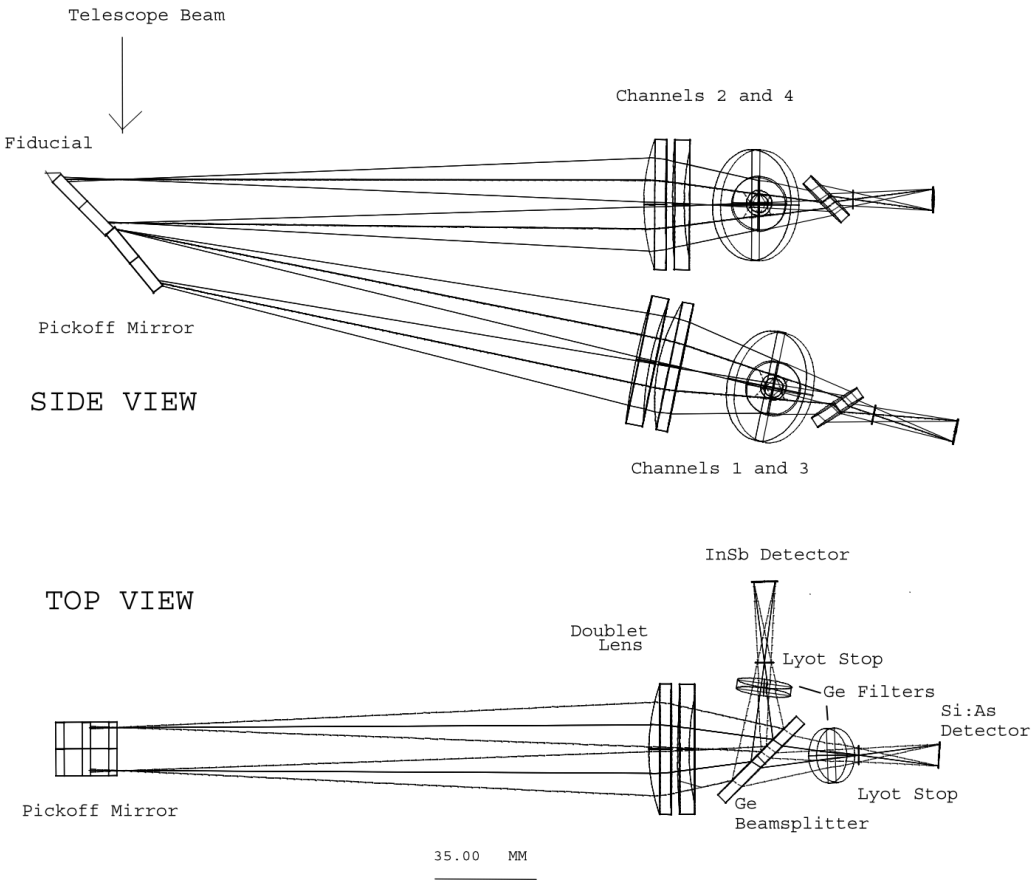

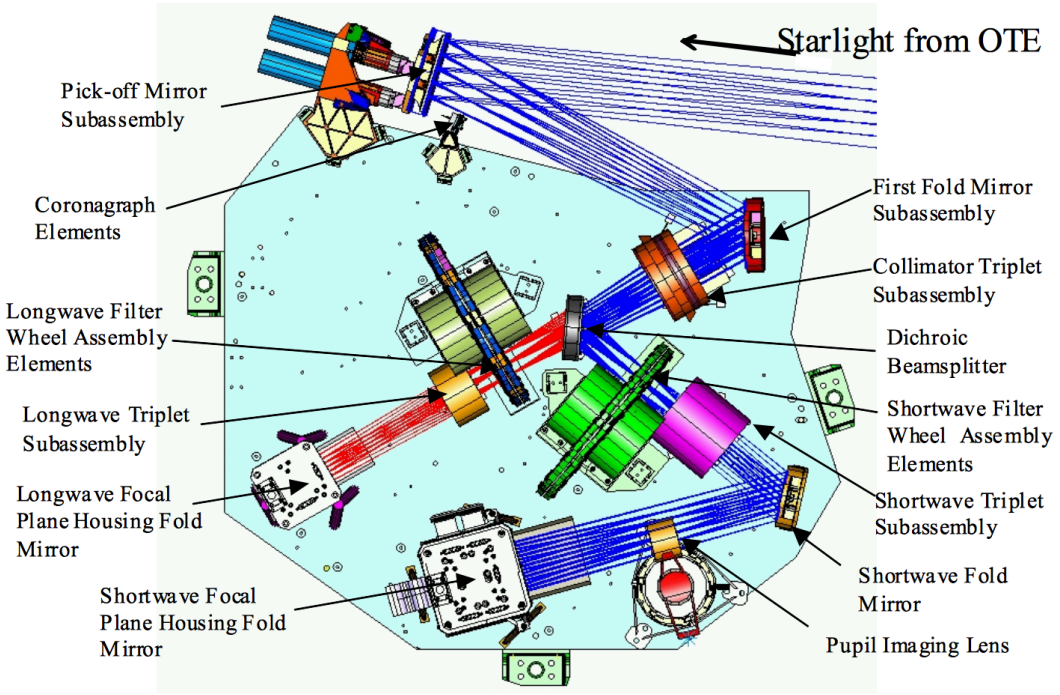

Fig. 1.— Optical Design of Spitzer IRAC (above) (Fazio et al. 2004) and JWST NIRCam (below) (Huff 2005)

in the images has to be filled by dithering moves.

2.3. Operation Mode

2.3.1. IRAC

The four 256×256 Focal Plane Arrays can be read out with different operation mode.They are full-array readout mode, stellar photometry mode and subarray mode.

In full-array readout mode, there were four selectable frame times: 2, 12, 30, and 100 s (Fazio et al. 2004). To allow sensitive observations without losing dynamic range, there was a high dynamic range option.

Stellar photometry mode was available for observations of objects much brighter in channels 1 and 2 than in 3 and 4 (typically stars). This mode took short exposures in channels 1 and 2, and long exposures in channels 3 and 4. The sensitivities of each frame are identical to those in full array mode.

For very bright sources, a subarray mode was available. In this mode, only a small 32×32 pixel portion of the array was read out, so the field of view was only $38' \times 38'$. Mapping was not allowed in subarray mode. In subarray readout mode, there were three selectable frame times: 0.02, 0.1, and 0.4 sec. This mode allows observer to catch fast variability of the targets (Fazio et al. 2004).

2.3.2. NIRCam

Comparing to IRAC, NIRCam equipped with more complicated devices, which allows different observation to be done.

The primary purpose of the NIRCam instrument is to take image measurement. For imaging observation, the major difference from IRAC is that both short wavelength and long wavelength channels of NIRCam are furnished with a Filter Wheel that allows for observations through more than 12 different spectral bands. There are totally 30 filters on NIRCam, whose wavelength covers from 0.7 to 4.8 μm.

Another unique feature of NIRCam is the ability to make Coronagraphic measurements. In coronagraphic mode, a coronagraphic occulting mask that can be chosen from a selection of sinc^2, top-hat, and Gaussian designs, optimized for light at either 2.0 or 4.6 μm blocks the light from the bright sources. This mode is essential in high contrast imaging observation, e.g. direct imaging of exoplanets.

NIRCam is also available for spectroscopic observation. NIRCam has a grism in the long wavelength channel. The grism offers the capability to carry out slitless spectroscopy in the wavelength range 2.4 to 5 μm, with spectroscopic resolution R $\sim$ 2000.

3. Instrument Performance

As a detector equipped on the next generation infrared space telescope, NIRCam definitely surpasses IRAC in different ways. Here I compare several key factors that most valued by exoplanet observation between IRAC and NIRCam to illustrate the great potential of NIRCam of expanding our horizon on exoplanet. There factors are spatial resolution, spectral coverage, sensitivity, and frame rate.

3.1. Spatial Resolution

High spatial resolution is essential to direct imaging observation. Limited by small size of primary mirror of Spitzer Space Telescope (0.85 m), it is not IRAC's strength to spatially resolve objects. The FWHMs of point spread functions (PSF) are $1''.66, 1''.72, 1''.88$and$1''.92$ at 3.6, 4.5, 5.8 and 8.0 μm channels, which are hugh for direct imaiging study. The large pixel scale ($1''.2$) resulting in under sampled PSF makes the situation even worse. As a result, IRAC is hardly ever used for imaging of wide orbit planetary mass companions.

The 6.5 m sized primary mirror of JWST provide NIRCam with significant spatial resolving ability. NIRCam's PSF has a FWHM of $0''.063$, which is nearly 20 times sharper than that of IRAC. The pixel scale that is optimized at 2 μm (Huff 2005) ensured well sampled PSFs at that wavelength. At smaller wavelength, the PSF would be a little undersampled. However the sample rate is still better than IRAC.

3.2. Wavelength Coverage

IRAC covers four wavelength channel at 3.6, 4.5, 5.8 and 8.0 μm. The wavelength coverage of NIRCam which ranges from 1 to 5 μm lacks long wave length ability comparing to IRAC. However, more than 30 filters supplied with NIRCam would provide spectral energy distribution with fine structures.

3.3. Sensitivity

Low thermal emission of exoplanets calls for high sensitivity. Table 1 and figure 2 illustrate the sensitivities of IRAC and NIRCam. In figure 2, sensitivities are expressed as the flux required to get 10 σ signal with a 10000 s exposure. Assuming $\sigma sim\sqrt{t}$, 10 σ signal

with 10000s exposure is generally equivalent to 1 σ signal with 100s exposure. Comparing to IRAC, NIRCam is more than 30 times sensible with wide band filter and more than 10 times sensible with narrow band filter.

3.4. Frame Rate

To catch the fast variability of a target, the detector is required to be read out fast. IRAC has an outstanding performance for high frame rate thanks to its subarray mode. It can be read out a 32×32 subarray for as fast as 0.02 s.

NIRCam also has the ability to read part of the full array out at a speed of 10 μs per pixel. Therefore to read the same size subarray as IRAC, it takes about 0.01 s, which is even shorter than what it takes for IRAC.

There are other factors that are related to exoplanet observation. For instance, high dynamic range that prevent the bright primary star image from severe saturation is essential to high contrast direct imaging observation. This point is not discussed here because IRAC is not suitable for such observation and NIRCam has coronagraphic element to overcome these problems, which makes it not comparable.

To sum, NIRCam has much better performance than IRAC in the aspects discussed above.

4. Application in Exoplanet

4.1. IRAC's Contribution in Exoplanet Observation

Initially, the most important in defining the IRAC design was the study of the early universe ((Fazio et al. 2004)). However, with the advantage in infrared wavelength coverage

Table 1. IRAC Sensitivity (1 σ, μJy), (Fazio et al. 2004)

Frame Time (s)	3.6μm	4.5μm	5.8μm	8.0μm
200	0.40	0.84	5.5	6.9
100	0.60	1.2	8.0	9.8
30	1.4	2.4	16	18
12	3.3	4.8	27	29
2	32	38	150	92
0.6	180	210	630	250
0.4	86	75	270	140
0.510	470	910	420	
0.02	7700	7200	11000	4900

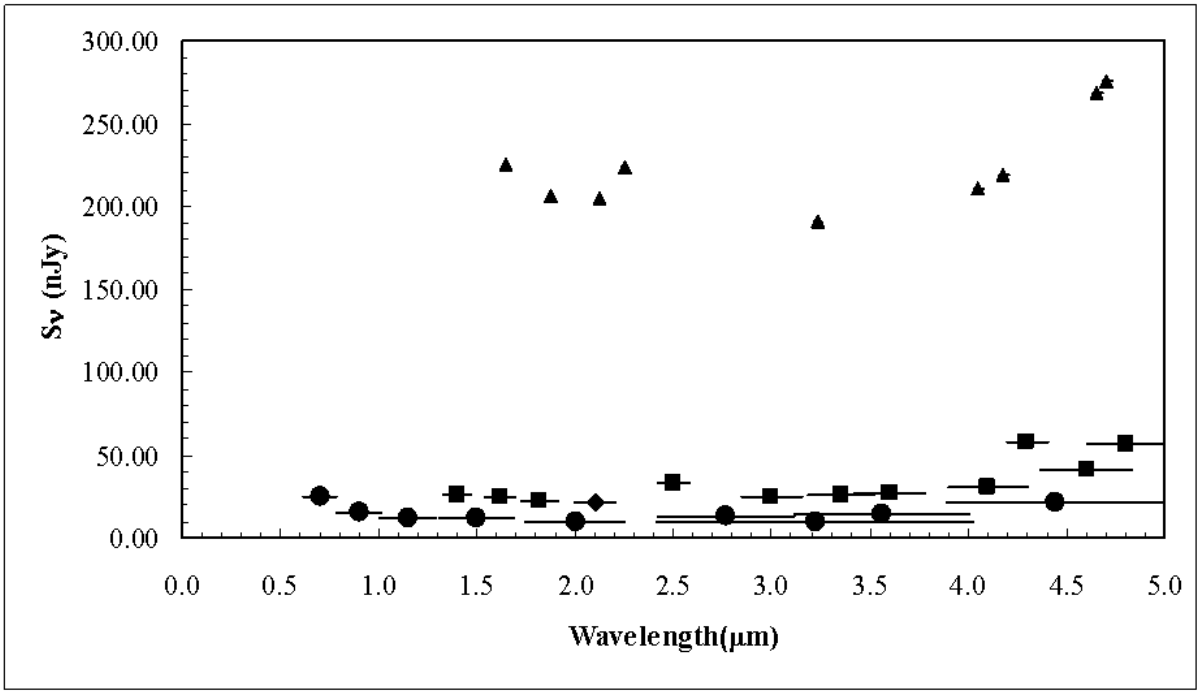

Fig. 2.— NIRCam Sensitivity (10 σ, exopsure time 10000s, nJy)

and high sensitivity, IRAC plays a great role in exoplanet observation. Although IRAC is limited by its design, e.g. the large FWHM of PSF is an obstacle for IRAC to carry out direct imaging of exoplanet, IRAC is the best devices for infrared transiting photometry before the launch of JWST.

Exoplanets' low surface temperatures locate their thermal emission peaks in infrared. Specially hot Jupiters whose effective temperatures are about 1000 K, are most ideal targets to detect thermal emission with. Charbonneau et al. (2005) took advantage of IRAC's high photometry precision to first detect the secondary eclipse of exoplanet TrES-1 which confirmed the thermal emission coming from the planet. They observed the target two channels, (4.5 and 8.0 μm), observed the field, and obtained 1518 full-array images in each of the two bandpasses (Charbonneau et al. 2005). The great accuracy of spitzer photometry data made it possible for them to construct the light curve that presented in figure 3 and detect the secondary eclipse dip.

In subarray mode, the high read out speed of IRAC is utilized to monitor the temporal variability of exoplanets. Knutson et al. (2007) observed HD189733 that is an eclipse planetary system containing a hot Jupiter and constructed a map of the distribution of temperatures by modeling the variability of the light curve. They monitored HD 189733 continuously over a 33.1 hour period using the 8 μm channel of IRAC in subarray mode with a cadence of 0.4 s. With the high cadence, high precision time series data (4), they saw a distinct rise in flux beginning shortly after the end of the transit and continuing until a time just prior to the beginning of the secondary eclipse, from which they created the map of exoplanet temperatures.

The combination of 4 channel photometries of IRAC could open a window for the study of exoplanet atmospheres (Burrows 2014). By comparing multi-band eclipse/secondary eclipse photometry with model spectrum, water and dust cloud feature can be traced (O'Donovan

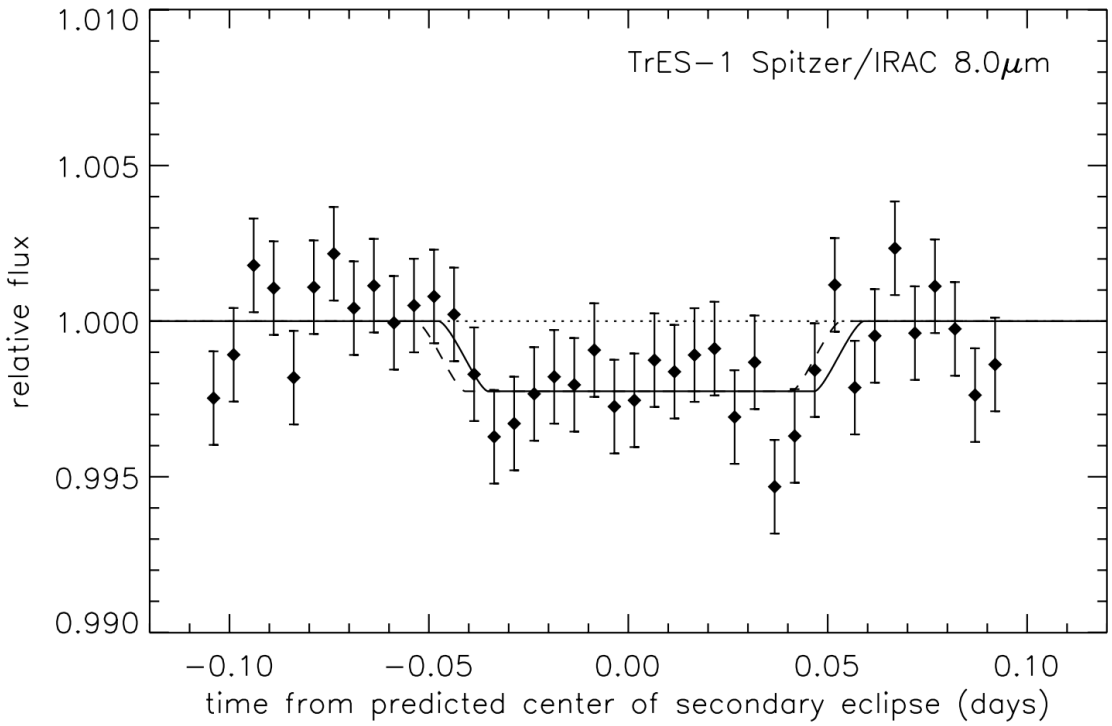

Fig. 3.— Light curve of TrES observed by IRAC Channel 4 (8μm) (Charbonneau et al. 2005).

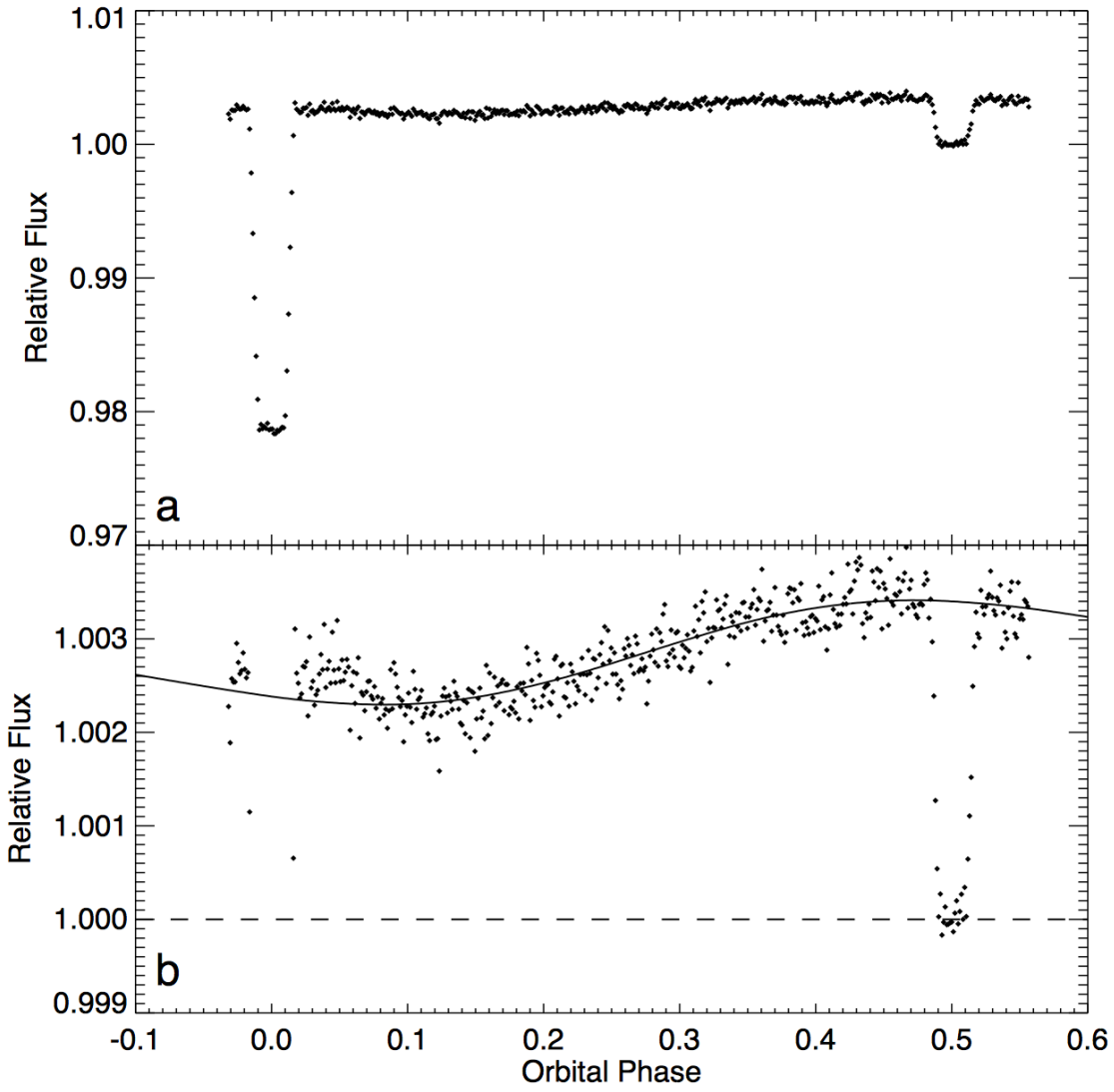

Fig. 4.— Light curve of high cadence observation of HD189733 system(Knutson et al. 2007).

et al. 2010).

4.2. NIRCam's Potential

§3 illustrates the great advantages of NIRCam in exoplanet observation. With the extraordinary work done with IRAC, we have reasons to expect NIRCam to make huge difference in this area of study.

4.2.1. Direct Imaging

Being different from IRAC that could only detect the thermal emission from exoplanet indirectly from secondary eclipse, NIRCam is able to directly take the image of exoplanets. The 6.5 m sized primary mirror and coronagraphic devices help NIRCam overcome two obstacles of direct imaging observation, small separation the planet from its host star and the high contrast in flux. With these barriers, today's direct imaging targets that are observed with ground based telescopes or HST are always on the boundary of planet and binary companions, whose masses are $\sim 10 M_{\rm Jul}$ and separations are more than 50 AU. However, a simulation for near by M star systems showed that NIRCam have the ability to detect Saturn-mass planet at ages of 1 Gyr or less located at a few 10s of AU from their host star (Beichman et al. 2012).

4.2.2. Transit Planet Study

NIRCam has significant strength in sensitivity. Higher signal to noise data liberate observation from the limit of the size and distance of the planets. NIRCam will be sensitive enough to confirm many of the small exoplanet candidates found by the Kepler mission to be

in the habitable zones of their host stars (Beichman et al. 2012). More fine structures would be uncovered in the transit light curve taken by NIRCam, allowing us to study properties such as limb darkening, oblateness and occultations of the transit planets more precisely.

Similar to IRAC, high frame rate in subarray read out mode let NIRCam catch fast variability of transit planets with much higher signal to noise. Great quality of data improves the confidence in mapping the surface temperature as well as clouds or hazes structures of the planets.

4.2.3. Exoplanet Spectroscopy

The most prominent advantage of NIRCam over IRAC is its multi-wavelength ability. The 4 channel IRAC observation is too coarse to identify any spectroscopic feature. However, more than 30 filters as well as the grism would totally reverse the situation.

For directed imaged planets, NIRCam allows grism observation to obtain the near infrared spectra of planetary mass companions to near by brown dwarfs (Green et al. 2005). Multi-band photometries and spectra would reveal information on accretion and formation history of exoplanets, which gives the answer to the question that how planets form. NIRCam grism observation could also study the jets from young T Tauri stars, which would disclose the sizes, excitations and column densities of such jets within 10 AU of nearby T Tauri stars, probing the radiation environments and gas densities of their planet-forming regions (Green et al. 2005).

Spectroscopic observation of transit planets is a powerful tool for planet atmosphere study. Figure 5 presents a simulation of exoplanet's atmosphere observed by JWST NIRSpec. NIRCam grism could provide low resolution spectra partially covering that region, which would act together with NIRSpec's high resolution spectra to help identify atmo-

sphere components of exoplanets.

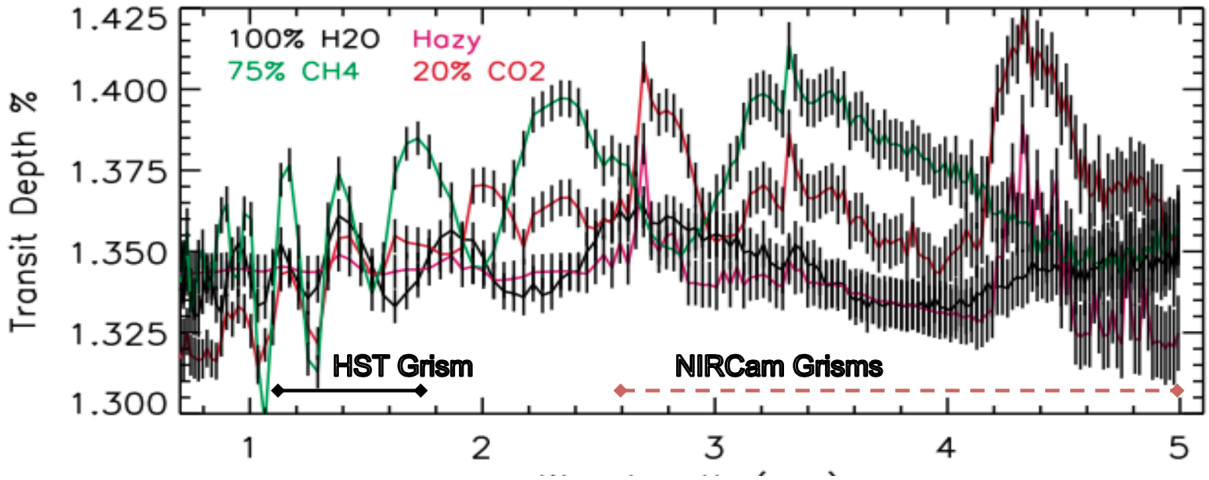

Fig. 5.— JWST NIRSpec prism simulation covers the wavelength range of NIRCam grism (Fortney et al. 2013). The low resolution NIRCam grism spectra would be very useful for identifying water, methane and haze components.

5. Summary

As the imaging device equipped on JWST, NIRcam exhibit its extraordinary power in spatial resolution, sensitivity, spectroscopic ability and read-out speed. NIRCam has significant advantages over IRAC in these aspects, which guarantees its great potential in exoplanet observations.

Frankly speaking, it is not for IRAC whose initial aim is to carry out deep, large-area surveys of $z > 3$ galaxy, to compare the ability of exoplanet observation ability with NIRCam who is optimized for exoplanet studies. However, since even an unoptimized instrument would make great discoveries, we should be reasonably confident about the future observations with NIRCam.

REFERENCES

C. A. Beichman, M. Rieke, D. Eisenstein, T. P. Greene, J. Krist, D. McCarthy, M. Meyer, and J. Stansberry. Science opportunities with the near-IR camera (NIRCam) on the James Webb Space Telescope (JWST). In *Society of Photo-Optical Instrumentation Engineers (SPIE) Conference Series*, volume 8442 of *Society of Photo-Optical Instrumentation Engineers (SPIE) Conference Series*, page 2, Sept. 2012. doi: 10.1117/12.925447.

L. G. Burriesci. NIRCam instrument overview. In J. B. Heaney and L. G. Burriesci, editors, *Cryogenic Optical Systems and Instruments XI*, volume 5904 of *Society of Photo-Optical Instrumentation Engineers (SPIE) Conference Series*, pages 21–29, Aug. 2005. doi: 10.1117/12.613596.

A. S. Burrows. Spectra as windows into exoplanet atmospheres. *Proceedings of the National Academy of Science*, 111:12601–12609, Sept. 2014. doi: 10.1073/pnas.1304208111.

D. Charbonneau, L. E. Allen, S. T. Megeath, G. Torres, R. Alonso, T. M. Brown, R. L. Gilliland, D. W. Latham, G. Mandushev, F. T. O'Donovan, and A. Sozzetti. Detection of Thermal Emission from an Extrasolar Planet. *ApJ*, 626:523–529, June 2005. doi: 10.1086/429991.

G. G. Fazio, J. L. Hora, L. E. Allen, M. L. N. Ashby, P. Barmby, L. K. Deutsch, J.-S. Huang, S. Kleiner, M. Marengo, S. T. Megeath, G. J. Melnick, M. A. Pahre, B. M. Patten, J. Polizotti, H. A. Smith, R. S. Taylor, Z. Wang, S. P. Willner, W. F. Hoffmann, J. L. Pipher, W. J. Forrest, C. W. McMurty, C. R. McCreight, M. E. McKelvey, R. E. McMurray, D. G. Koch, S. H. Moseley, R. G. Arendt, J. E. Mentzell, C. T. Marx, P. Losch, P. Mayman, W. Eichhorn, D. Krebs, M. Jhabvala, D. Y. Gezari, D. J. Fixsen, J. Flores, K. Shakoorzadeh, R. Jungo, C. Hakun, L. Workman, G. Karpati,

R. Kichak, R. Whitley, S. Mann, E. V. Tollestrup, P. Eisenhardt, D. Stern, V. Gorjian, B. Bhattacharya, S. Carey, B. O. Nelson, W. J. Glaccum, M. Lacy, P. J. Lowrance, S. Laine, W. T. Reach, J. A. Stauffer, J. A. Surace, G. Wilson, E. L. Wright, A. Hoffman, G. Domingo, and M. Cohen. The Infrared Array Camera (IRAC) for the Spitzer Space Telescope. *ApJS*, 154:10–17, Sept. 2004. doi: 10.1086/422843.

J. J. Fortney, C. Mordasini, N. Nettelmann, E. M.-R. Kempton, T. P. Greene, and K. Zahnle. A Framework for Characterizing the Atmospheres of Low-mass Low-density Transiting Planets. *ApJ*, 775:80, Sept. 2013. doi: 10.1088/0004-637X/775/1/80.

J. J. Green, C. Beichman, S. A. Basinger, S. Horner, M. Meyer, D. C. Redding, M. Rieke, and J. T. Trauger. High contrast imaging with the JWST NIRCAM coronagraph. In D. R. Coulter, editor, *Techniques and Instrumentation for Detection of Exoplanets II*, volume 5905 of *Society of Photo-Optical Instrumentation Engineers (SPIE) Conference Series*, pages 185–195, Aug. 2005. doi: 10.1117/12.619343.

J. L. Hora, M. Marengo, R. Park, D. Wood, W. F. Hoffmann, P. J. Lowrance, S. J. Carey, J. A. Surace, J. E. Krick, W. J. Glaccum, J. G. Ingalls, S. Laine, G. G. Fazio, M. L. N. Ashby, and Z. Wang. The IRAC point response function in the warm Spitzer mission. In *Society of Photo-Optical Instrumentation Engineers (SPIE) Conference Series*, volume 8442 of *Society of Photo-Optical Instrumentation Engineers (SPIE) Conference Series*, page 39, Sept. 2012. doi: 10.1117/12.926894.

L. W. Huff. NIRCam instrument optics. In J. B. Heaney and L. G. Burriesci, editors, *Cryogenic Optical Systems and Instruments XI*, volume 5904 of *Society of Photo-Optical Instrumentation Engineers (SPIE) Conference Series*, pages 30–37, Aug. 2005. doi: 10.1117/12.619909.

H. A. Knutson, D. Charbonneau, L. E. Allen, J. J. Fortney, E. Agol, N. B. Cowan, A. P.

Showman, C. S. Cooper, and S. T. Megeath. A map of the day-night contrast of the extrasolar planet HD 189733b. *Nature*, 447:183–186, May 2007. doi: 10.1038/nature05782.

J. E. Krist, C. A. Beichman, J. T. Trauger, M. J. Rieke, S. Somerstein, J. J. Green, S. D. Horner, J. A. Stansberry, F. Shi, M. R. Meyer, K. R. Stapelfeldt, and T. L. Roellig. Hunting planets and observing disks with the JWST NIRCam coronagraph. In *Society of Photo-Optical Instrumentation Engineers (SPIE) Conference Series*, volume 6693 of *Society of Photo-Optical Instrumentation Engineers (SPIE) Conference Series*, page 0, Sept. 2007. doi: 10.1117/12.734873.

F. T. O'Donovan, D. Charbonneau, J. Harrington, N. Madhusudhan, S. Seager, D. Deming, and H. A. Knutson. Detection of Planetary Emission from the Exoplanet Tres-2 Using Spitzer/IRAC. *ApJ*, 710:1551–1556, Feb. 2010. doi: 10.1088/0004-637X/710/2/1551.